Journal of Applied Mechanics and Technical Physics, Vol. 49, No. 5, pp. 749–753, 2008

NUMERICAL SIMULATION OF AXISYMMETRIC TURBULENT JETS

A. G. Demenkov[1], B. B. Ilyushin[1,3], and G. G. Chernykh[2,3]

UDC 532.517.4

The flow in axisymmetric turbulent jets is numerically simulated with the use of a semi-empirical second-order turbulence model including differential transport equations for the normal Reynolds stresses. Calculated results are demonstrated to agree with experimental data.

Key words: *axisymmetric turbulent jet, differential transport equations for the Reynolds stresses, finite-difference method, numerical simulation.*

Introduction. The dynamics of a circular turbulent jet, which is the classical problem of experimental, theoretical, and computational fluid dynamics, has been studied in many papers (see [1–14] and the references therein). The flow in circular turbulent jets at significant distances from the sources was studied in experiments [1, 8]. The experiments [1] were performed at a Reynolds number $\mathrm{Re} = U_{\mathrm{jet}} D/\nu = 10^5$ determined on the basis of the jet velocity U_{jet} and nozzle diameter D with $x/D = 30$–100; the experiments [8] were performed at $\mathrm{Re} = 1.1 \cdot 10^4$ and $x/D = 30$–160. The experiments [1, 8] were performed by different techniques, and the examined jets exhibit differences in a number characteristic parameters. Possibly, this is the reason for different interpretations of the data obtained. Amielh et al. [9] performed experiments to study the flow dynamics in the near field of turbulent jets of gases with different densities (non-self-similar regimes) in a co-flow, and the data obtained were compared with the results [1, 8]. Laboratory measurements were performed at $\mathrm{Re} = 2.1 \cdot 10^4$ and $x/D = 0$–30. Gharbi et al. [10] reported results of numerical simulations of circular turbulent jets obtained by using a model including transport equations for all components of the Reynolds stress tensor and dissipation rate of the turbulent kinetic energy. The calculated results are shown to be consistent with the experimental data [9]. Piquet [11] performed a detailed analysis of data obtained in experimental and theoretical (including numerical) studies of such flows. Ilyushin and Krasinsky [14] performed a numerical study of a free circular turbulent submerged jet by the large eddy simulation (LES) method; the conditions of experiments [12, 13] were modeled, the calculated and measured characteristics of turbulence were compared, and the influence of the model constants and parameters of the numerical algorithm on the accuracy of calculations was analyzed.

Though various turbulent jet flows have been studied in much detail, some issues have not be addressed. In particular, numerical models of axisymmetric jet flows are not complete. Numerical simulations performed in [10, 14] were compared with experimental data in the near field of the jet. Piquet [11] reviewed the results of numerical analyses of the flow under the test conditions [1, 2] performed with the use of several semi-empirical models of turbulence. As far as we are aware, no numerical simulations of the flow in the far field were performed on the basis of the experimental data [8], which are the most complete ones. There is no unified mathematical model that would allow both the near field ($x/D \leqslant 30$) and the far field ($x/D \geqslant 30$) to be calculated. The present paper is aimed at filling these gaps.

[1]Kutateladze Institute of Thermophysics, Siberian Division, Russian Academy of Sciences, Novosibirsk 630090; demenkov@itp.nsc.ru. [2]Institute of Computational Technologies, Siberian Division, Russian Academy of Sciences, Novosibirsk 630090; ilyushin@itp.nsc.ru. [3]Novosibirsk State University, Novosibirsk 630090; chernykh@ict.nsc.ru. Translated from Prikladnaya Mekhanika i Tekhnicheskaya Fizika, Vol. 49, No. 5, pp. 55–60, September–October, 2008. Original article submitted June 6, 2007; revision submitted September 4, 2007.

1. Formulation of the Problem. The flow is described with the use of the following system of averaged equations (boundary-layer approximation):

$$U\,\frac{\partial U}{\partial x}+V\,\frac{\partial U}{\partial r}=-\frac{1}{r}\,\frac{\partial}{\partial r}\,r\langle u'v'\rangle; \tag{1}$$

$$\frac{\partial U}{\partial x}+\frac{\partial V}{\partial r}+\frac{V}{r}=0. \tag{2}$$

Here (x, r, φ) is a cylindrical coordinate system with the origin on the nozzle exit, U, V, u', v', and w' are the corresponding components of velocity of the mean and fluctuating motion, and $\langle u'v'\rangle$ is the Reynolds shear stress; the averaging is denoted by broken brackets. In the right side of Eq. (1), the term including molecular viscosity is assumed to be small and, hence, is omitted. The sought functions do not depend on the φ coordinate, because the jets considered are axisymmetric.

System (1), (2) is not closed. The turbulent shear stress is determined from the known Rodi's relations [2, 5]

$$\langle u'v'\rangle=\lambda\langle v'^2\rangle\,\frac{\partial U}{\partial r},\qquad \lambda=-\frac{1-C_2}{C_1-1+P/\varepsilon}\,\frac{e}{\varepsilon}. \tag{3}$$

The normal Reynolds stresses ($2e=\langle u'^2\rangle+\langle v'^2\rangle+\langle w'^2\rangle$) and the dissipation rate ε are found from the transport equations:

$$U\,\frac{\partial\langle u'^2\rangle}{\partial x}+V\frac{\partial\langle u'^2\rangle}{\partial r}=-2(1-\alpha)\langle u'v'\rangle\,\frac{\partial U}{\partial r}-\frac{2}{3}\,\varepsilon-C_1\,\frac{\varepsilon}{e}\Big(\langle u'^2\rangle-\frac{2}{3}\,e\Big)+\frac{2}{3}\,\alpha P+\frac{C_s}{r}\,\frac{\partial}{\partial r}\Big(\frac{re\langle v'^2\rangle}{\varepsilon}\,\frac{\partial\langle u'^2\rangle}{\partial r}\Big); \tag{4}$$

$$U\,\frac{\partial\langle v'^2\rangle}{\partial x}+V\,\frac{\partial\langle v'^2\rangle}{\partial r}=-\frac{2}{3}\,\varepsilon-C_1\,\frac{\varepsilon}{e}\Big(\langle v'^2\rangle-\frac{2}{3}e\Big)+\frac{2}{3}\,\alpha P$$
$$+\frac{C_s}{r}\,\frac{\partial}{\partial r}\,\frac{re}{\varepsilon}\,\langle v'^2\rangle\,\frac{\partial\langle v'^2\rangle}{\partial r}-\frac{2C_se}{r\varepsilon}\,\langle w'^2\rangle\,\frac{\langle v'^2\rangle-\langle w'^2\rangle}{r}; \tag{5}$$

$$U\,\frac{\partial\langle w'^2\rangle}{\partial x}+V\,\frac{\partial\langle w'^2\rangle}{\partial r}=-\frac{2}{3}\,\varepsilon-C_1\,\frac{\varepsilon}{e}\Big(\langle w'^2\rangle-\frac{2}{3}\,e\Big)+\frac{2}{3}\,\alpha P$$
$$+\frac{C_s}{r}\,\frac{\partial}{\partial r}\,\frac{re}{\varepsilon}\,\langle v'^2\rangle\,\frac{\partial\langle w'^2\rangle}{\partial r}+\frac{2C_se}{r\varepsilon}\,\langle w'^2\rangle\,\frac{\langle v'^2\rangle-\langle w'^2\rangle}{r}; \tag{6}$$

$$U\,\frac{\partial\varepsilon}{\partial x}+V\,\frac{\partial\varepsilon}{\partial r}=\frac{C_\varepsilon}{r}\,\frac{\partial}{\partial r}\,\frac{re}{\varepsilon}\,\langle v'^2\rangle\,\frac{\partial\varepsilon}{\partial r}+\Big(C_{\varepsilon1}\,\frac{P}{\varepsilon}-C_{\varepsilon2}\Big)\frac{\varepsilon^2}{e}. \tag{7}$$

The expression for the turbulent energy production P in (3)–(7) has the form

$$P=-\langle u'v'\rangle\,\frac{\partial U}{\partial r}.$$

The mathematical model used in the present work is close to the model described in [15, 16], where a swirling turbulent wake behind a self-propelled body was studied; the present model is a simplification of the latter model to a non-swirling flow. The model structure is caused by anisotropy of turbulence degeneration in the jet.

In equations and relations (3)–(7), the quantities C_s, C_ε, α, C_1, C_2, $C_{\varepsilon1}$, and $C_{\varepsilon2}$ are empirical constants. We used their standard values [5, 6]: $C_s=0.22$, $C_\varepsilon=0.17$, $\alpha=0.6$, $C_1=2$, $C_2=0.6$, $C_{\varepsilon1}=1.45$, and $C_{\varepsilon2}=1.92$. For $x=x_0$, the initial conditions were set in the form of distributions of U, $\langle u'^2\rangle$, $\langle v'^2\rangle$, $\langle w'^2\rangle$, and ε correlated with experimental data. The initial values of ε were determined from the known Kolmogorov's relation $\varepsilon=\gamma e^{3/2}/r_{1/2}$, where $r_{1/2}$ is found from the equality $e(x_0, r_{1/2})=e(x_0, 0)/2$ and γ is an empirical constant. As $r\to\infty$, either an undisturbed flow or a co-flow was modeled. For an undisturbed flow, the values of U, $\langle u'^2\rangle$, $\langle v'^2\rangle$, $\langle w'^2\rangle$, and ε were assumed to be equal to zero. In modeling a co-flow, the von Neumann condition was imposed for these variables. At $r=0$, the sought quantities satisfied the conditions

$$\frac{\partial U}{\partial r}=\frac{\partial\langle u'^2\rangle}{\partial r}=\frac{\partial\langle v'^2\rangle}{\partial r}=\frac{\partial\langle w'^2\rangle}{\partial r}=\frac{\partial\varepsilon}{\partial r}=V=0.$$

The initial and boundary conditions for $\langle v'^2\rangle$ and $\langle w'^2\rangle$ are such that $\langle v'^2\rangle\equiv\langle w'^2\rangle$.

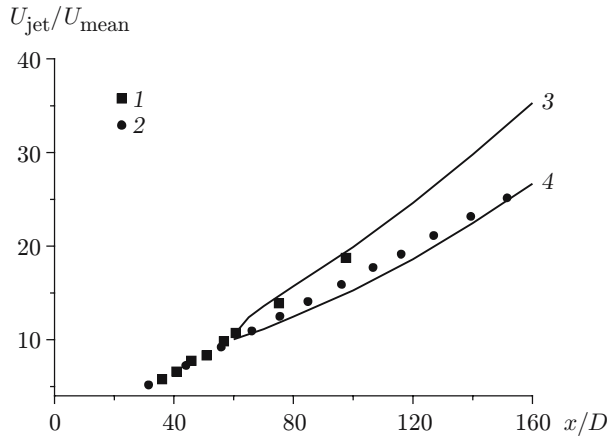

Fig. 1. Axial values of the mean velocity along the centerline U_c: curves 1 and 3 are obtained with $\text{Re} = 10^5$ and $x/D = 30$–100 (curve 1 shows the experimental data [1] and curve 3 shows the calculated results); curves 2 and 4 are obtained with $\text{Re} = 1.1 \cdot 10^4$ and $x/D = 30$–160 (curve 2 shows the experimental data [8], and curve 4 shows the calculated results).

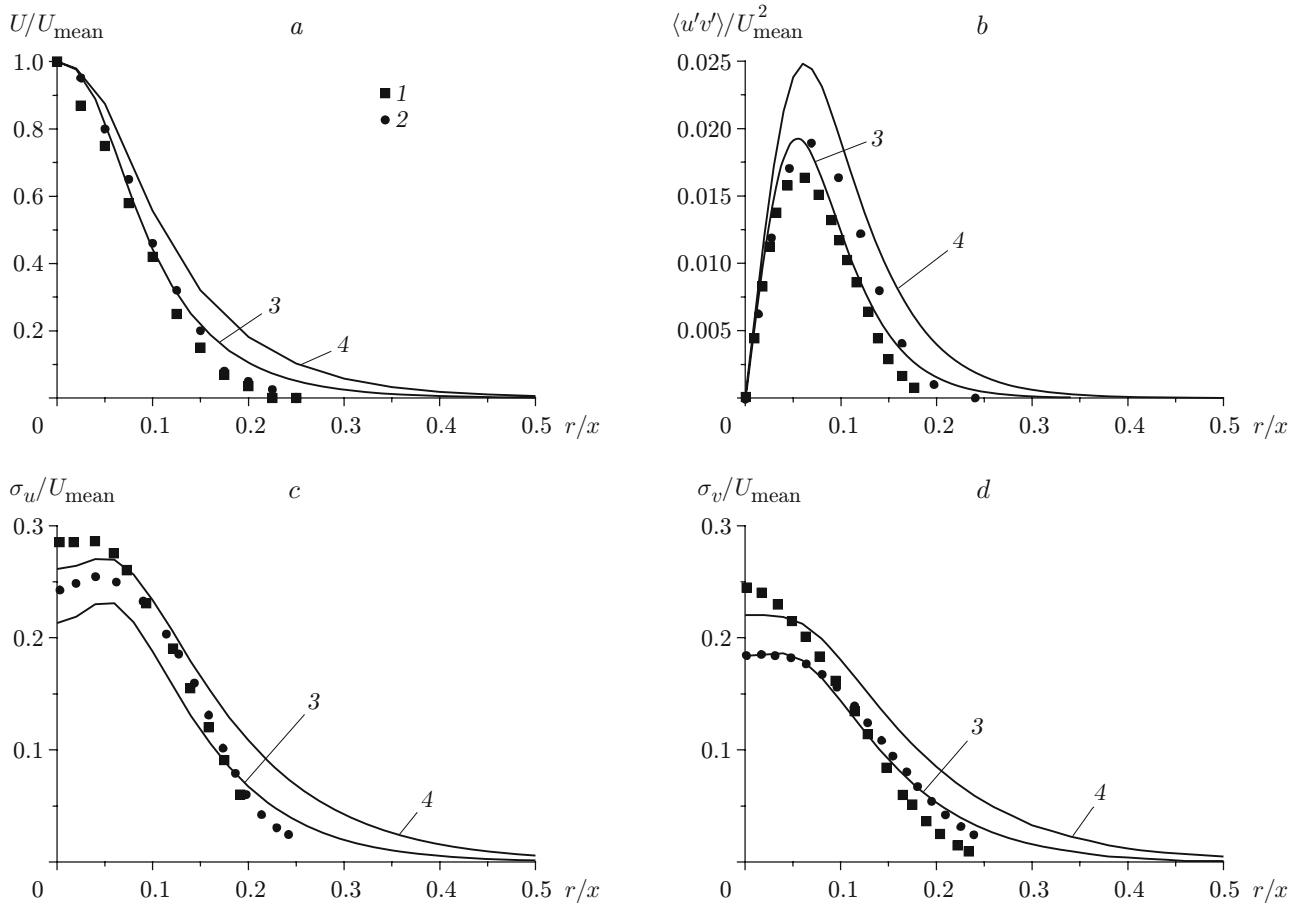

Fig. 2. Radial profiles of the mean streamwise velocity component U (a), Reynolds shear stress $\langle u'v' \rangle$ (b), and intensities σ_u and σ_v of turbulent fluctuations of velocity components (c and d): curves 1 and 3 are obtained with $x/D = 100$ (curve 1 shows the experimental data [1], and curve 3 shows the results calculated with the initial conditions from [1]); curves 2 and 4 are obtained with $x/D = 160$ (curve 2 shows the experimental data [8], and curve 4 shows the results calculated with the initial conditions from [8]).

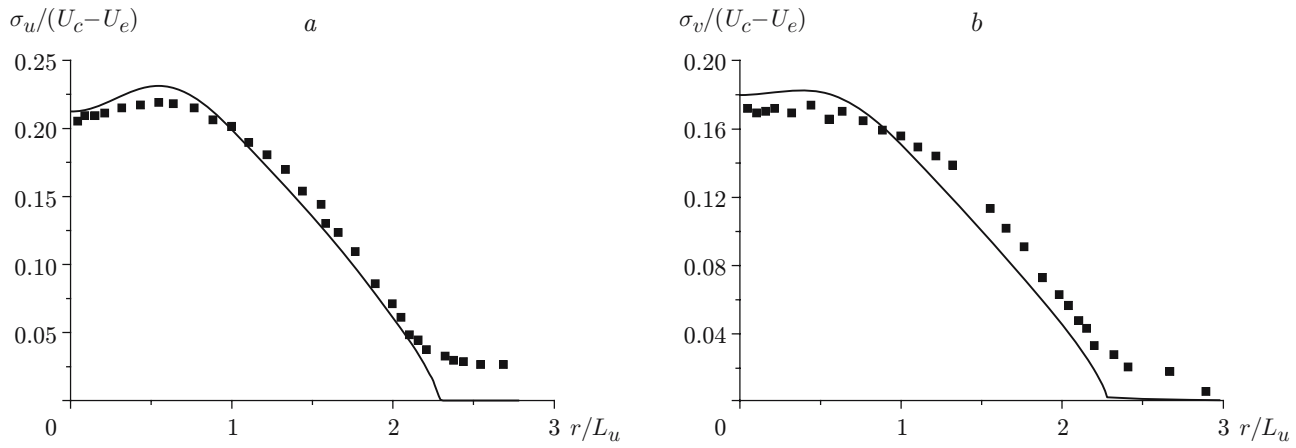

Fig. 3. Radial profiles σ_u (a) and σ_v (b) for $x/D = 20$: the points are the experimental data [9], and the curves are the calculated results.

The variables in the problem can be normalized by using the scales of the axial velocity of the jet at the nozzle exit U_{jet} and the characteristic length D (nozzle diameter).

In the numerical solution, we passed to the variable ψ [$rU = \partial\psi/\partial r$ and $-rV = \partial\psi/\partial x$], introduced a uniform grid, and applied implicit finite-difference schemes with iterations in terms of nonlinearity. The algorithm of problem solution is conservative in terms of the law of conservation of momentum; it was tested in detail in [16].

In simulating the test conditions [1, 8] and [9], the boundary conditions were shifted from infinity to a rather far-away boundary: $r/D = 100$ and $r/D = 10$, respectively. For the initial conditions [1, 8], the step of the difference grid was chosen to be $h_x/D = 0.005$ for the variable x and $h_r/D = 0.2$ for the spatial variable. The calculations of the near field of the jet flow [9] were performed for $h_x/D = 5 \cdot 10^{-5}$ and $h_r/D = 0.02$. Reduction of these parameters by a factor of 2 led to deviations in the grid analog of the norm of the space of continuous functions smaller than 1%.

2. Calculation Results. The first series of numerical experiments was performed for the far field of the jet [1, 8]. The initial conditions in the calculations were set at $x/D = 60$, because the experimental profiles of the normal Reynolds stresses and the mean streamwise velocity component were not given in [1, 8] for smaller distances. The calculated and experimentally measured axial values of the mean streamwise velocity component are plotted in Fig. 1 (the notation from [1, 8] is used in Figs. 1 and 2). The calculated results are seen to be in reasonable agreement with the experimental data.

The transverse distributions of the streamwise velocity component U, Reynolds shear stress $\langle u'v'\rangle$, and intensities of turbulent fluctuations of the horizontal component of velocity ($\sigma_u = \sqrt{\langle u'^2\rangle}$) and vertical component of velocity ($\sigma_v = \sqrt{\langle v'^2\rangle}$) are plotted in Fig. 2. The calculated results agree with the experimental data.

To study the behavior of the turbulent jet characteristics at large distances from the nozzle exit, we performed a numerical experiment where we analyzed the changes in the calculated characteristic scales of turbulence $\sqrt{e_0}/U_c$, U_0/U_c, L_U/D, and L_e/D, depending on the distance. The length scales were found from the relations

$$L_U\colon \quad U(x, L_U) = \frac{1}{2}\,U(x, 0) = \frac{1}{2}\,U_0, \qquad L_e\colon \quad e(x, L_e) = \frac{1}{2}\,e(x, 0) = e_0.$$

For $x/D \geqslant 500$, the decay laws were found to be close to the known classical decay laws $U_c \sim x^{-1}$, $\sqrt{e_0} \sim x^{-1}$, $L_U \sim x^1$, and $L_e \sim x^1$. Affine similarity of the transverse distributions of the corresponding functions was observed; for the initial conditions [1, 8], these functions almost coincided. The behavior of the ratio of the turbulent energy production to its dissipation rate P/ε was also analyzed. It turned out that the maximum value of this quantity stays in the interval $P/\varepsilon \in (0.80, 0.95)$ and almost does not decrease with increasing distance. For comparison, it is worth noting that the maximum value in a swirling turbulent wake behind a self-propelled body [16] is $P/\varepsilon \approx 0.3$ at $x/D = 20$, and its value decreases with increasing distance from the body.

The next series of numerical experiments was performed on the basis of the experimental data [9], where the flow in the near field of a turbulent jet was studied. In the calculations, the initial conditions were imposed at

$x/D = 14$. An attempt to impose initial conditions at smaller distances from the nozzle yielded significant errors caused, apparently, by the boundary-layer approximation used in this work.

Figure 3 shows the calculated and measured transverse distributions of intensities of velocity fluctuations σ_u and σ_v for $x/D = 20$ (U_e is the co-flow velocity). The calculated results are in reasonable agreement with the experimental data. In addition, reasonable agreement with the experimental data [9] is reached in terms of degeneration of the axial values of the intensities σ_u and σ_v, mean velocity U, jet half-width L_u, and transverse distributions $\langle u'v' \rangle$.

As was noted above, the mathematical model considered is a simplified modification of the mathematical model described in [15, 16] for the case of non-swirling jet flows. Without any additional calibration, the model provides a detailed description of the jet flow and the swirling turbulent wake flow behind a self-propelled body. Thus, semi-empirical models of turbulence are fairly universal.

Conclusions. A numerical model of the dynamics of a turbulent axisymmetric jet is constructed with the use of a mathematical model including differential transport equations of the normal Reynolds stresses. The calculated results are in reasonable agreement with experimental data both for the near field and for the far field of the jet flow.

This work was supported by the Russian Foundation for Basic Research (Grant Nos. 06-01-00724-a and 07-01-00363-a).

REFERENCES

1. I. Wygnanski and H. Fiedler, "Some measurements in the self-preserving jet," *J. Fluid Mech.*, **38**, 577–612 (1969).
2. W. Rodi, "The prediction of free turbulent boundary layers by use of two-equation model of turbulence," Ph. D. Thesis, London (1972).
3. W. Frost and T. Moulden (eds.), *Handbook of Turbulence. V. 1. Fundamentals and Applications*, Plenum Press, New York–London (1977).
4. J. A. Schetz, "Injection and mixing in turbulent flow," in: *Progress in Astronautics and Aeronautics*, Vol. 68, New York Univ., New York (1980).
5. W. Rodi, *Turbulence Models and Their Application in Hydraulics*, Univ. of Karlsruhe, Karlsruhe (1980).
6. B. E. Launder and A. Morse, "Numerical prediction of axisymmetric free shear flows with a second-order Reynolds stress closure," in: F. Durst, B. E. Launder, F. W. Schmidt, and J. N. Whitelaw (eds.), *Turbulent Shear Flows*, Springer, Berlin (1979), pp. 279–294.
7. G. N. Abramovich, T. A. Girshovich, S. Yu. Krashenninnikov, A. N. Sekundov, and I. P. Smirnova, *Theory of Turbulent Jets* [in Russian], Nauka, Moscow (1984).
8. N. R. Panchapakesan and J. L. Lumley, "Turbulence measurements in axisymmetric jets of air and helium. Part 1. Air jet," *J. Fluid Mech.*, **246**, 197–223 (1993).
9. M. Amielh, T. Djeridane, F. Anselmet, and L. Fulachier, "Velocity near-field of variable density turbulent jets," *Int. J. Heat Mass Transfer*, **39**, No. 10, 2149–2164 (1996).
10. A. Gharbi, E. Ruffin, F. Anselmet, and R. Schiestel, "Numerical modelling of variable density turbulent jets," *Int. J. Heat Mass Transfer*, **39**, No. 9, 1865–1882 (1996).
11. J. Piquet, *Turbulent Flows: Models and Physics*, Springer-Verlag, Berlin–Heidelberg (1999).
12. S. V. Alekseenko, A. V. Bilsky, and D. M. Markovich, "Application of the method of digital tracer visualization for analyzing turbulent flow with a periodic component," *Prib. Tekh. Éksp.*, No. 5, 145–153 (2004).
13. S. V. Alekseenko, A. V. Bilsky, V. M. Dulin, et al., "Non-intrusive determination of turbulent energy balance in free and confined jet flows," in: *Proc. of the 4th Int. Symp. on Turbulence and Shear Flow Phenomena* (TSFP-4), Williamsburg, June 27–29 (2005), pp. 605–610.
14. B. B. Ilyushin and D. V. Krasinsky, "Large eddy simulation of the turbulent round jet dynamics," *Thermophys. Aeromech.*, **13**, No. 1, 43–54 (2006).
15. O. F. Vasil'ev, A. G. Demenkov, V. A. Kostomakha, and G. G. Chernykh, "Numerical simulation of a swirling turbulent wake behind a self-propelled body," *Dokl. Ross. Akad. Nauk*, **376**, No. 2, 195–1999 (2001).
16. G. G. Chernykh, A. G. Demenkov, and V. A. Kostomakha, "Swirling turbulent wake behind a self-propelled body," *Int. J. Comput. Fluid Dynamics*, **19**, No. 5, 370–379 (2005).